Opportunistic use of catecholamine neurotransmitters as siderophores to access iron by Pseudomonas aeruginosa

Quentin Perraud, Lauriane Kuhn, Sarah Fritsch, Gwenaëlle Graulier, Véronique Gasser, Vincent Normant, Philippe Hammann, Isabelle Schalk

environmental microbiology
environmental microbiology reports

Opportunistic use of catecholamine neurotransmitters as siderophores to access iron by Pseudomonas aeruginosa

Journal:	*Environmental Microbiology and Environmental Microbiology Reports*
Manuscript ID	EMI-2020-1831.R1
Journal:	Environmental Microbiology
Manuscript Type:	EMI - Research article
Date Submitted by the Author:	n/a
Complete List of Authors:	Perraud, Quentin; Université de Strasbourg, ESBS, UMR7242 Kuhn, Lauriane; CNRS FRC1589, Institut de Biologie Moléculaire et Cellulaire Fritsch, Sarah; University of Strasbourg, ESBS, UMR7242 Graulier, Gwenaëlle; Université de Strasbourg, ESBS, UMR7242 Gasser, Véronique; Université de Strasbourg, UMR7242 Normant, Vincent; Université de Strasbourg, ESBS, UMR7242 Hammann, Philippe; CNRS FRC1589, Institut de Biologie Moléculaire et Cellulaire Schalk, Isabelle; Université de Strasbourg, ESBS, UMR7242; Université de Strasbourg, ESBS, UMR7242
Keywords:	siderophore, iron uptake, Pseudomonas aeruginosa, catecholamine, neurotransmitter, outer membrane transporter, TonB dependent transporter, infection

Opportunistic use of catecholamine neurotransmitters as siderophores to access iron by *Pseudomonas* aeruginosa

Quentin PERRAUD[a,b], Lauriane KUHN[c], Sarah FRITSCH[a,b], Gwenaëlle GRAULIER[a,b], Véronique Gasser[a,b], Vincent Normant[a,b], Philippe HAMMANN[c], and Isabelle J. SCHALK[a,b*]

[a] Université de Strasbourg, UMR7242, ESBS, Bld Sébastien Brant,
F-67413 Illkirch, Strasbourg, France

[b] CNRS, UMR7242, ESBS, Bld Sébastien Brant,
F-67413 Illkirch, Strasbourg, France

[c] Plateforme Proteomique Strasbourg - Esplanade, Institut de Biologie Moléculaire et Cellulaire, CNRS, FR1589, 15 rue Descartes, F-67084 Strasbourg Cedex.

[*] To whom correspondence should be addressed: schalk@unistra.fr.

Running title: *P. aeruginosa* cells use catecholamines to access iron

ABSTRACT

Iron is an essential nutrient for bacterial growth and the cause of a fierce battle between the pathogen and host during infection. Bacteria have developed several strategies to access iron from the host, the most common being the production of siderophores, small iron-chelating molecules secreted into the bacterial environment. The opportunist pathogen *Pseudomonas aeruginosa* produces two siderophores, pyoverdine and pyochelin, and is also able to use a wide panoply of xenosiderophores, siderophores produced by other microorganisms. Here, we demonstrate that catecholamine neurotransmitters (dopamine, L-DOPA, epinephrine, and norepinephrine) are able to chelate iron and efficiently bring iron into *P. aeruginosa* cells *via* TonB-dependent transporters (TBDTs). Bacterial growth assays under strong iron-restricted conditions and with numerous mutants showed that the TBDTs involved are PiuA and PirA. PiuA exhibited more pronounced specificity for dopamine uptake than for norepinephrine, epinephrine, and L-DOPA, whereas PirA specificity appeared to be higher for L-DOPA and norepinephrine. Proteomic and qRT-PCR approaches showed *pirA* transcription and expression to be induced in the presence of all four catecholamines. Finally, the oxidative properties of catecholamines enable them to reduce iron, and we observed ferrous iron uptake via the FeoABC system in the presence of L-DOPA.

INTRODUCTION

Iron availability is very low for bacteria during infection due to the sequestration of iron by host proteins, such as transferrin, lactoferrin and ferritin. Thus, most bacteria access iron by relying on the production and secretion of siderophores, low molecular weight organic compounds with an extremely high affinity for ferric iron (Hider and Kong, 2011). These compounds scavenge iron from the bacterial environment before being transported back into bacteria via outer-membrane transporters, of which the uptake activity is regulated by an interaction with an inner-membrane protein called TonB (Schalk and Guillon, 2013). These outer-membrane transporters are commonly called TonB-dependent transporters (TBDT).

Siderophores produced by bacteria can have widely varying chemical structures, but all chelate ferric iron via either catecholate, hydroxamate, carboxylate functions, salicylate or heterocycle (Hider and Kong, 2011). The most highly studied siderophores are probably the tris-catecholates, which include the archetypal siderophore enterobactin (Pollack and Neilands, 1970; O'Brien and Gibson, 1970), as well as protochelin, corynebactin, salmochelin, and bacillibactin (Cornish and Page, 2000; May *et al.*, 2001; Bluhm *et al.*, 2002; Müller *et al.*, 2009). These siderophores behave as hexadentate ligands that can chelate ferric iron through the hydroxyl moieties of their three catechol functions, forming octahedral complexes (Raymond *et al.*, 2003).

Catecholate-containing molecules also have major functions in metazoans, with, for example, catecholamines, such as dopamine, norepinephrine, and epinephrine, acting as neurotransmitters in vertebrates (Eisenhofer *et al.*, 2004). However, they also exhibit a wide array of functions across all kingdoms, to the extent that they have been hypothesized to be

part of an ancient evolutionary chemical language used by all life forms, much like the genetic code (Roshchina, 2016). Although the question of the evolutionary origin of catecholamines remains unresolved, it is clear that this class of molecules is ancient and widespread. Indeed, in mammals, they are not confined solely to the central nervous system but can be found in the gastrointestinal tract, peripheral sympathetic nerve endings, and bloodstream (Eisenhofer *et al.*, 2004).

The existence of a link between catecholamines and infection was proposed after the observation of a correlation between high levels of circulating catecholamines and serious infections (Groves *et al.*, 1973; Jones *et al.*, 1988). Cases of sepsis have been noted from the beginning of the therapeutic use of purified adrenaline in the 1940s (Cooper, 1946; Evans *et al.*, 1948). The first hypotheses concerning this link concerned the immunomodulatory role of adrenaline and norepinephrine, until Lyte and Ernst studied the impact of neurotransmitters on bacterial growth and virulence in the 1990s (Lyte and Ernst 1992; Lyte et al. 1997). The ability of catecholamines to stimulate growth and enhance virulence appears to be widespread among both Gram-negative and Gram-positive bacteria (Verbrugghe *et al.*, 2012). One hypotheses to explain this effect is the detection of catecholamines by two-component systems, thus allowing the pathogen to recognize an abnormal inflammatory state in their host (Reading *et al.*, 2009; Hughes *et al.*, 2009). Another is that catecholamines may be used as siderophores or agents to facilitate the acquisition of iron by pathogens, as these molecules are capable to form ferric complexes via their catechol group (Siraki *et al.*, 2000; Dichtl *et al.*, 2019). Consistent with this second hypothesis, it has been shown that *Bacillus subtilis* (Miethke and Skerra, 2010), *Bordetella bronchiseptica* (Anderson and Armstrong, 2008), and *E. coli* (Burton *et al.*, 2002) are able to use norepinephrine for iron import. *Bacillus subtilis* assimilates norepinephrine-Fe through

the ferrous iron uptake pathway FeuABC (Miethke and Skerra, 2010). Moreover, norepinephrine-Fe has been shown to facilitate iron acquisition from transferrin in *Bordetella bronchiseptica* in a TonB-dependent fashion and activate the transcription of the enterobactin TBDT *bfeA* (Anderson and Armstrong, 2008). In addition, the enterohemorrhagic strain of *Escherichia coli* O157:H7 is able to sense the presence of epinephrine and norepinephrine in its environment through the QseC/B two-component system involved in quorum sensing (Hughes *et al.*, 2009) and displays increased iron acquisition in the presence of both norepinephrine and transferrin (Freestone *et al.*, 2003). At last, more recently, it was shown that the solute binding lipoprotein PiuA from the Fe acquisition ABC transporter PiuBCDA, binds tetradentate norepinephrine-Fe complexes, (Zhang *et al.*, 2020).

Despite recent interest in metabolic crosstalk between microorganisms and their hosts (Belkaid and Hand, 2014; Yoo *et al.*, 2020), very little information is available concerning the clinically relevant pathogen *P. aeruginosa.* The few studies undertaken have demonstrated that the PA14 strain shows increased virulence when cultivated with norepinephrine, a result that could be replicated by adding $FeCl_3$ to the culture medium, suggests a link between norepinephrine and an increase in bacterial intracellular iron concentrations (Hegde *et al.*, 2009). It has been proposed that catecholamines have the ability to facilitate iron scavenging from transferrin by reducing iron(III) to soluble iron(II), for which transferrin has a very low affinity (Sandrini *et al.*, 2010). However, *P. aeruginosa* has been shown to be capable of scavenging iron from transferrin without the assistance of such molecules, as the ability to produce the high-affinity siderophore pyoverdine and protease elastase is sufficient (Doring *et al.*, 1988; Meyer *et al.*, 1996). Consequently, it is still unknown whether

112 catecholamine involvement in iron acquisition is biologically relevant or whether the
113 observations described above were artifacts caused by the limitation of available models.
114 No attempts have yet been made to determine whether ferric forms of catecholamine
115 compounds can enter *P. aeruginosa* cells and directly provide this opportunistic pathogen
116 with iron. This pathogen is able to import ferrous iron (Fe^{2+}) via the FeoABC uptake system,
117 access heme using three heme acquisition pathways, and access ferric iron (Fe^{3+}) using
118 siderophores (Cornelis and Dingemans, 2013). *P. aeruginosa* produces two siderophores,
119 pyoverdine (PVD) and pyochelin (PCH) (Schalk *et al.*, 2020), but it is also able to use
120 numerous siderophores produced by other bacteria present in its environment in a
121 "siderophore piracy" strategy (Cornelis and Dingemans, 2013; Perraud *et al.*, 2020). *P.*
122 *aeruginosa* has in its genome 34 genes encoding TBDTs, with twelve of them being involved
123 in iron acquisition (Winsor *et al.*, 2016). For a third of these transporters, the siderophore or
124 molecule transported has not been identified.
125 Here, we show that dopamine, L-DOPA, epinephrine, and norepinephrine (Figure 1) are all
126 able to chelate iron. ^{55}Fe uptake assays, bacterial growth tests under iron-restricted
127 conditions, and the use of numerous mutants showed that these molecules transport iron in
128 *P. aeruginosa* cells via the TBDTs PirA and PiuA. Proteomic and qRT-PCR approaches also
129 showed that *pirA* transcription and expression is stimulated by the presence of
130 catecholamines in the bacterial environment, also indicating that PirA is involved in iron
131 acquisition via catecholamine compounds. Finally, ferrous uptake was also observed in the
132 presence of L-DOPA, involving the FeoABC system.

RESULTS

Catecholamines chelate iron via their catechol function. Catecholamines are known to form complexes with iron (Melin *et al.*, 2015), but their affinity for iron is unknown. We used the CAS-Fe (Chrome azurol S) test, developed by Neilands and Schwyn (Schwyn and Neilands, 1987), to assess the ability of several catecholamines to chelate iron (Figure 1). In this test, the ternary complex chrome azurol S-Fe^{3+}-hexadecyltrimethylammonium bromide, with absorbance at 630 nm, serves as an indicator (Schwyn and Neilands, 1987), as its color changes from blue to orange when a strong chelator removes the iron from the dye. Dopamine, L-DOPA, epinephrine, and norepinephrine were able to scavenge iron from CAS with equivalent efficiency, whereas normetanephrine, an O-methylated structural analogue of norepinephrine, was not (Figure 2A). These data confirm that catecholamines are able to chelate iron(III) through their catechol moiety. Comparison of the ability of catecholamines to scavenge iron from CAS with that of pyoverdine or pyochelin (the two siderophores produced by *P. aeruginosa* to access iron (Schalk *et al.*, 2020)) clearly showed these monocatechol-containing compounds to have a much lower affinity for iron than the two siderophores produced by *P. aeruginosa* (ka of 10^{32} M^{-1} and 10^{18} M^{-2} for pyoverdine and pyochelin respectively (Albrecht-Gary *et al.*, 1994; Brandel *et al.*, 2012)). Comparison of the ability to scavenge iron from CAS between the catecholamines themselves showed norepinephrine to have the highest affinity, followed by epinephrine, dopamine, and L-DOPA.

We also tested the ability of these catecholamines to compete for iron with pyoverdine. Apo pyoverdine is fluorescent at 447 nm (excitation at 400 nm) and this fluorescence is quenched when the siderophore chelates iron (Schalk *et al.*, 2002; Folschweiller *et al.*, 2002). We used this spectral property to compare the ability of the catecholamines to remove iron

158 from 10 µM pyoverdine-Fe (Perraud *et al.*, 2020). The same assay was also carried out using
159 a previously described tris-catechol compound (TCV), which has an ability to compete for
160 iron with pyoverdine similar to that of the tris-catechol enterobactin produced by *E. coli*
161 (Gasser *et al.*, 2016). As previously described, TCV efficiently removed iron from pyoverdine:
162 all 10 µM of pyoverdine was in the apo form in the presence of 17 µM of TCV (Figure 2B).
163 Norepinephrine, dopamine, and epinephrine were clearly less efficient than TCV in this
164 competition assay: 20 mM of these mono-catechols removed iron from only 20 to 25% of
165 the 10 µM of ferri-pyoverdine present in the assay. Normetanephrin was unable to scavenge
166 iron from pyoverdine, which was expected as this molecule is O-methylated. L-DOPA was
167 unable to remove iron from pyoverdine-Fe but was able to do so from CAS-Fe (Figure 2A),
168 indicating that L-DOPA has a lower affinity for iron than norepinephrine, dopamine, and
169 epinephrine.
170 Overall, these data show that norepinephrine, dopamine, epinephrine, and L-DOPA are able
171 to chelate iron but with affinities clearly lower than those of pyoverdine and siderophores
172 such as tris-catechols.
173
174 **Catecholamines are able to reduce Fe^{3+} to Fe^{2+} at physiological pH.** Catecholamines are
175 easily oxidized in the presence of Lewis acids such as Fe^{3+}. Thus, we investigated whether
176 catecholamines can reduce Fe^{3+} to Fe^{2+} using ferrozine, a specific Fe^{2+} chelator that forms a
177 stable magenta-colored complex solely with Fe^{2+}, with a specific absorption peak at 562 nm
178 (Stookey, 1970). Incubation of the catecholamines with Fe^{3+} and ferrozine resulted in a slow
179 increase in absorbance at 562 nm, corresponding to ferrozine-Fe^{2+} formation, for all
180 molecules except normetanephrine (Figure 2C). The ability of ferrozine to trap Fe^{2+} indicates
181 that a fraction of Fe^{3+} was reduced to Fe^{2+} in the presence of catecholamines other than

normetanephrine. However, this fraction only represented approximately 10% of the Fe^{3+} reduced by dithiothreitol (DTT), and the kinetics of reduction were also much slower than that observed with DTT. The inability of normetanephrine to reduce iron was certainly due to O-methylation of the catechol function.

Catecholamines are able to promote ^{55}Fe-acquisition by P. aeruginosa. We followed the kinetics of ^{55}Fe accumulation by *P. aeruginosa* cells incubated in the presence of catecholamine-^{55}Fe complexes to determine whether dopamine, L-DOPA, epinephrine, and norepinephrine are able to promote iron assimilation by the bacteria (Figure 3). The uptake assays were carried out using a *P. aeruginosa* strain that is unable to produce pyoverdine or pyochelin (Δ*pvdF*Δ*pchA*, Table 1SM in Supplemental Materials) to ensure that the observed transport of iron was due to the catecholamines and not the siderophores produced by the bacteria. We included a control condition in which the strain Δ*pvdF*Δ*pchA* was preincubated with the proton-motive force inhibitor carbonyl cyanide-m-chlorophenylhydrazone (CCCP) for each of the catecholamines tested. This made it possible to distinguish TonB-dependent transport from nonspecific interactions with the bacterial cell surface or diffusion of complexed-^{55}Fe into the bacteria through porins. Indeed, as CCCP inhibits the inner membrane proton gradient, it blocks any transport involving TBDTs (Clément *et al.*, 2004). Moreover, *P. aeruginosa* cells are able to sense the presence of siderophores produced by other bacteria (xenosiderophores) in their environment and, in response, express the proteins (among others the TBDTs) required to access iron via these xenosiderophores (Llamas *et al.*, 2006; Llamas *et al.*, 2008; Perraud *et al.*, 2020). Such a mechanism may also exist for catecholamines. Thus, the bacteria used in this ^{55}Fe uptake assay were grown in

CAA (iron-restricted medium) in the presence of 10 µM of one of the four catecholamines to induce the expression of the potential proteins needed to access iron via these molecules.

We observed ^{55}Fe accumulation over time for all four catecholamines (Figure 3), with an efficiency of approximately 40% of that of pyoverdine (pyoverdin-^{55}Fe uptake was carried out in parallel, Fig 1SM in Supplemental Materials) and of the same order as that we previously observed for ferrichrome ((Normant *et al.*, 2020), an xenosiderophore used by *P. aeruginosa*).

Except for dopamine, ^{55}Fe uptake was largely inhibited in the presence of CCCP, indicating that the observed transport is dependent on the proton gradient of the bacterial inner membrane and is thus TonB-dependent, as for any iron uptake by siderophores. Furthermore, the inhibition of ^{55}Fe accumulation by CCCP in the presence of epinephrine, L-DOPA, or norepinephrine also rules out reduction of ferric to ferrous iron during the 3 h of the uptake assay, as it is more soluble and can either diffuse into bacteria or be imported by the FeoABC system.

For dopamine, the accumulation of ^{55}Fe was independent of the inner-membrane proton gradient (Figure 3), indicating either diffusion of the complex into the bacteria, a nonspecific interaction of the ferric complex with the bacterial cell surface, or the reduction of iron followed by diffusion or uptake by the inner membrane FeoAB transporter. A study of the effects of dopamine in the context of the pathophysiology of Parkinson's disease showed the ability of this compound to form adducts with peroxidized fatty acids via its primary amine (Liu *et al.*, 2008), which could explain our ^{55}Fe assimilation data. However, we cannot exclude that such a nonspecific interaction or the diffusion of dopamine-^{55}Fe through porins did not mask weak TonB-dependent transport. Indeed, the amount of ^{55}Fe associated with bacteria was slightly higher for dopamine than the other molecules tested.

We next attempted to identify the TBDT(s) involved in iron acquisition by these catecholamines. We used a *P. aeruginosa* strain that is unable to produce pyoverdine or pyochelin and mutated for several TBDTs involved in iron uptake via catechol-type siderophores (Δ*pvdF*Δ*pchA*Δ*pfeA*Δ*pirA*Δ*piuA*Δ*fvbA*Δ*PA0434*, Table 1SM in Supplementary materials). This mutant is deleted for: *pfeA* and *pirA*, two TBDTs involved in ferri-enterobactin uptake (Ghysels *et al.*, 2005); *piuA*, a TBDT involved in the uptake of BAL30072-Fe, a siderophore-beta-lactam compound developed by Basilea (Moynié *et al.*, 2017)); *fvbA*, a TBTD involved in the uptake of ferri-vibriobactin, a tris-catechol type siderophore (Elias *et al.*, 2011)), and PA0434, a TBTD for which the siderophore has not been identified but for which the expression is induced by the presence of ferri-viriobactin (Perraud *et al.*, 2020). Deletion of none of these five genes had an effect on the iron uptake kinetics using epinephrine, norepinephrine, dopamine, or L-DOPA as chelators, suggesting either the involvement of none of these TBDTs in this biological process or the involvement of several TBDT(s). The involvement of several TBDTs in the import of iron by a siderophore has also been shown for pyoverdine (FpvA and FpvB, (Ghysels *et al.*, 2004)), enterobactin (PfeA and PirA, (Ghysels *et al.*, 2005), ferrichrome (FiuA and another unidentified TBDT, (Normant *et al.*, 2020)), and desferioxamine (FoxA and another unidentified TBDT (Normant *et al.*, 2020)). One TBDT can take over uptake if the other is not expressed.

In conclusion, these data clearly show that L-DOPA, epinephrine, norepinephrine, and dopamine are able to promote iron transport into *P. aeruginosa* cells that are unable to produce pyoverdine or pyochelin and that such transport is clearly TonB-dependent for L-DOPA, epinephrine, and norepinephrine and apparently not for dopamine. However, we were unable to identify the transporters involved using this approach.

The presence of catecholamines in P. aeruginosa growth media induces the expression of the TBDT PirA. As already mentioned above, *P. aeruginosa*, like many other bacterial species, is able to use siderophores produced by other bacteria (xenosiderophores) to access iron, in a strategy called siderophore piracy (Traxler *et al.*, 2012; Galet *et al.*, 2015). This goes hand in hand with the presence of at least one gene in the bacterial genome encoding a TBDT for each xenosiderophore that can be used, as well as, genes encoding inner-membrane transporters and enzymes involved in xenosiderophore-iron dissociation mechanisms. The transcription of these genes are often upregulated by the presence of the xenosiderophores themselves in the bacterial environment (Dean *et al.*, 1996; Llamas *et al.*, 2006; Llamas *et al.*, 2008; Llamas *et al.*, 2014), and can be easily followed using a differential proteomic approach that we previously developed (Perraud *et al.*, 2020). Thus, we studied the adaptation of the proteome of *P. aeruginosa* to the presence of 10 µM of the catecholamines or normetanephrine. For these experiments, we used a strain that is unable to produce pyoverdine or pyochelin (Δ*pvdF*Δ*pchA*), as the catecholamines have a low affinity for iron and compete poorly with pyoverdine for iron chelation (Figures 2A and 2B).

Cells were grown in iron-restricted casaminoacid medium (CAA medium, iron concentration of 20 nM according to previous work of our team (Cunrath *et al.*, 2016)), with or without one of the five compounds tested, and analyzed by proteomics and RT-qPCR. The proteomic data (Figure 4) show very strong induction of the expression of the TBDT PirA in the presence of epinephrine, as well as weaker induction of the expression of this transporter in the presence of norepinephrine and L-DOPA. PirA has been described in the literature as a secondary TBDT for iron uptake by enterobactin in *P. aeruginosa* (Ghysels *et al.*, 2005). Neither normetanephrine nor dopamine were able to induce the expression of this transporter, consistent with the observation that normetanephrine is unable to chelate

277 ferric iron and dopamine to carry out a TonB-dependent transport of iron. We also observed
278 a slight decrease in the expression of the ferric citrate-transporter FecA in the presence of
279 dopamine, epinephrine, and L-DOPA. No strong repression of the expression of the various
280 proteins involved in pyoverdine and pyochelin (the two siderophores produced by *P.*
281 *aeruginosa*) uptake pathways was observed.
282 RT-qPCR (qualitative reverse transciption polymerase chain reaction) (Figure 5) confirmed
283 that epinephrine, norepinephrine, and L-DOPA are able to induce the transcription of *pirA,*
284 whereas normetanephrine is not. Dopamine also appeared to slightly induce *pirA*
285 transcription, but apparently with a level of protein synthesis that was not detected by the
286 proteomic approach. We also observed increased transcription of *feoB*, a gene involved in
287 the assimilation of iron(II), for dopamine, L-DOPA, epinephrine, and normetanephrine, but
288 there was no detectable induction of the expression of the FeoAB system by differential
289 proteomics. Normetanephrine is unable to bind or reduce ferric iron. Thus, the observed
290 increase in *feoB* transcription may not be associated with the induction of these genes by
291 the catecholamines to import the ferrous iron produced by these chelators. Surprisingly, the
292 transcription of *fecA* was not significantly reduced, in contrast to the results obtained by
293 differential proteomics. We also observed a decrease in the transcription of *fptA*, the gene
294 encoding the TBDT for pyochelin, in the presence of epinephrine and norepinephrine,
295 indicating that these two compounds apparently compete more efficiently for iron with
296 pyochelin than L-DOPA or dopamine. Finally, the transcription of *fpvA,* the TBDT of the
297 pyoverdine pathway, was not repressed because none of the catecholamines tested were
298 able to compete for iron with this siderophore.
299 Overall, these data show that the presence of epinephrine, norepinephrine, L-DOPA, or, to a
300 lower extent, dopamine in the bacterial growth media induces the transcription and

301 expression of the TBDT PirA, suggesting that this transporter is involved in iron assimilation
302 by these compounds in *P. aeruginosa* cells. The induction was the strongest with
303 epinephrine. In addition, as *pirA* transcription is regulated by a two-component system
304 (PirS/PirR), the ferri-catecholamine complex is necessarily able to interact with the sensor
305 PirS, located in the cytoplasmic membrane, demonstrating an ability of the molecules to
306 cross the outer membrane of *P aeruginosa* and activate the sensor at the inner membrane
307
308 **Deletion of *piuA* and, to a lower extent, *pirA* strongly inhibits bacterial growth in the**
309 **presence of catecholamines.** Epinephrine, norepinephrine, and L-DOPA appear to induce
310 PirA expression. Thus, we sought to determine whether the deletion of *pirA*, and eventually
311 other genes encoding TBDTs, would have an inhibitory effect on *P. aeruginosa* grown in iron-
312 restricted conditions in the presence of catecholamines. As already described, we performed
313 the growth test in iron-restricted growth medium (CAA medium), in which mutants with
314 gene deletions are routinely tested: if a gene deletion leads to growth inhibition, the
315 mutated gene is involved in iron assimilation. In this test, we used the mutants Δ*pvdF*Δ*pchA*
316 (unable to produce the siderophores pyoverdine and pyochelin) and a corresponding
317 collection of mutants deleted for genes encoding TBDTs (Table 1SM in Supplementary
318 Materials). The various strains were grown in CAA medium in the absence or presence of 10
319 µM of one of the catecholamine compounds or normetanephrine. Only the data of mutants
320 showing growth inhibition are presented in Figure 6. Surprisingly, deletion of *pirA* (strain
321 Δ*pvdF*Δ*pchA*Δ*pirA*, Table 1SM) had no impact on the growth of *P. aeruginosa* in the presence
322 of catecholamines, despite the induction of transcription and expression of this gene
323 observed by proteomics and qRT-PCR, indicating that at least one other transporter can
324 perform ferri-catecholamine uptake when PirA is not expressed.

Surprisingly, this experiment revealed 60% inhibition of bacterial growth for the *piuA* mutant (Δ*pvdF*Δ*pchA*Δ*piuA*) in the presence of dopamine, a delay in growth in the presence of L-DOPA, epinephrine and norepinephrine, and no effect when normetanephrine was present. These data indicate that PiuA is involved in iron acquisition via catecholamine compounds and, despite the data obtained when following ^{55}Fe uptake, dopamine also appears to transport iron via a TBDT. The fact that normetanephrine, the O-methylated catecholamine analogue, had no impact on Δ*pvdF*ΔpchAΔ*piuA* growth strongly suggests that the observed growth inhibition or delay was directly dependent on the iron-chelating or iron-reducing properties of the four other catecholamines. PiuA is a TBDT for which the natural ligand(s) have not been yet identified. Based on *P. aeruginosa* genome *piuA* transcription, it is not regulated by a sigma factor or two-component system and therefore cannot be induced by the presence of the catecholamine molecules, unlike *pirA* (Winsor *et al.*, 2016). Altogether, our results indicate, that PiuA is involved in the uptake of iron by epinephrine, norepinephrine, dopamine, and L-DOPA. PiuA in *P. aeruginosa* is a TBDT and not a solute binding lipoprotein associated to the ABC transporter PiuBCDA as in *Streptococcus pneumoniae* (Zhang *et al.*, 2020), both proteins have the same name but to not belong to the same protein family.

Catecholamines are easily oxidized and their quinone derivatives are potentially disruptive to redox systems. Thus, we also verified that the growth impairment we observed with the *piuA* mutation was not due to hypothetical hypersensitivity to oxidative stress of the strains, but rather to the sequestration of iron by the catecholamines, rendering the nutrient unusable by the bacteria because their transporter, PiuA, was not expressed. We therefore grew the Δ*pvdF*Δ*pchA* and Δ*pvdF*Δ*pchA*Δ*piuA* strains, either in the presence of one of the catecholamines or in the presence of one of the catecholamines and enterobactin, a very

strong iron chelator. Enterobactin is a tris-catechol siderophore that displays one of the highest known affinities for iron(III) amongst siderophores ($K_d = 10^{-52}$ M, (Harris *et al.*, 1979) and would easily be able to out-compete catecholamines for iron. In the presence of enterobactin, the catecholamines would theoretically be unable to compete for iron chelation and consequently no further iron acquisition should occur via PiuA but only via PfeA and PirA, the two TBDTs of ferri-enterobactin (Dean and Poole, 1993; Ghysels *et al.*, 2005). We observed no significant differences in growth between the two conditions for Δ*pvdF*Δ*pchA* cells, either in the presence of only catecholamines or catecholamines and enterobactin. As expected, we observed almost no growth of the Δ*pvdF*Δ*pchA*Δ*piuA* mutant in the presence of the catecholamines alone, but the growth was restored by enterobactin, because the bacteria could access iron via this siderophore and its transporters, PfeA and PirA. This confirms that the inhibitory effect observed in the presence of catecholamines for the *piuA*-deleted strain was due to the inability of the bacteria to access the iron pool chelated by catecholamines and not oxidative stress.

We observed further growth inhibition for dopamine and norepinephrine when both *piuA* and *pirA* were deleted, reaching the 60% inhibition observed with L-DOPA on Δ*pvdF*Δ*pchA*Δ*piuA*, suggesting that PirA is involved in iron acquisition via at least these two molecules. As growth inhibition was not complete for the double *piuA* and *pirA* mutant, especially for epinephrine, a third TBDT is likely be involved in iron assimilation via catecholamine compounds. Deletion of *pfeA*, the enterobactin TBDT, had no additional inhibitory effect (growth with Δ*pvdF*Δ*pchA*Δ*piuA*Δ*pirA*Δ*pfeA*). We also compared the growth between Δ*pvdF*Δ*pchA*Δ*piuA* and Δ*pvdF*Δ*pchA*Δ*piuA*Δ*feoABC* strains, *feoABC* consisting of the three genes involved in ferrous iron uptake, to assess ferrous iron uptake in the presence of

372 the catecholamines. There was an additional effect for L-DOPA only, suggesting that this
373 compound may reduce iron, which is then transported by the FeoABC system.
374 In conclusion, PiuA is involved in iron assimilation mostly via dopamine but also, at a lower
375 level via norepinephrine, L-DOPA and epinephrine. PirA appears to be more highly involved
376 in iron uptake via L-DOPA and norepinephrine. Finally, iron is apparently also weakly
377 transported by FeoAB in the presence of L-DOPA.
378

DISCUSSION

Catecholamines have already been reported to be capable of facilitating iron acquisition from transferrin (Sandrini *et al.*, 2010), but nothing is known about the possible use of catecholamines as siderophores for iron uptake by *P. aeruginosa*. Our data show that *P. aeruginosa* is able to use catecholamines to acquire this metal under iron-restricted conditions, even in the absence of proteins such as transferrin, through the use of TBDTs, as observed for all siderophores in Gram-negative bacteria. The growth assay we used under strong iron-restricted conditions with a Δ*pvdF*Δ*pchA* strain and its corresponding TBDT mutants show that both the TBDTs PirA and PiuA are involved in this uptake process (Figure 7). PiuA appears to be more specific to dopamine but is also able to transport iron-loaded epinephrine, norepinephrine, and L-DOPA, whereas PirA appears to be more specific to L-DOPA and norepinephrine. Finally, ferrous iron is also apparently weakly transported by the ferrous iron transporter FeoAB in the presence of L-DOPA. Deletion of *piuA*, *pirA*, and *feoB* did not completely abolish iron uptake by catecholamines, suggesting that (i) one other TBDT is also involved, (ii) that catecholamines-Fe complexes diffusion via porins, especially in the case of dopamine, or (iii) that Fe^{3+} is rapidly exchanged with other ligands in the growth media like citrate.

The identification of the *piuA* gene in the importation of ferri-catecholamine complexes into *P. aeruginosa* cells provides information concerning the ligand selectivity of this TBDT. To date, the only molecules described in the literature to be recognized by PiuA are the synthetic sideromycins BAL30072 and MC-1 from the pharmaceutical industry (Moynié *et al.*, 2017). These sideromycins are based on vectorization by monohydroxypyridones,

403 considered to be analogues of monocatechols. PiuA may play a key role in iron acquisition
404 via catecholamines by the pathogen during infections.
405
406 The induction of transcription and expression of *pirA* in the presence of catecholamines
407 indicates that this TBDT is able to import iron-loaded catecholamines into *P. aeruginosa* cells
408 and that these compounds are able to interact with the two component system PirS/PirR
409 (PirS being the inner-membrane sensor and PirA the transcriptional regulator (Llamas *et al.*,
410 2008)) (Figure 7). As PirS is located in the inner membrane, catecholamines have to reach
411 the bacterial periplasm to interact with this sensor and activate the transcription of *pirA*. Our
412 proteomic results can also explain the induction of *pirA* transcription observed in *P.*
413 *aeruginosa* cells in an acute murine pneumonia infection model: not only was the
414 transcription of *pirA* induced, but also proteins of the pyoverdine and heme uptake
415 pathways (Damron *et al.*, 2016). These results suggest that *P. aeruginosa* is able to use
416 catecholamines as siderophores during an infection via the PirA transporter.
417
418 A surprising result in our data was the non-involvement of the tris-catechol enterobactin and
419 the vibriobactin TBDTs, PfeA, PirA, and FvbA, in the importation of the iron complexes of
420 epinephrine, norepinephrine, dopamine, and L-DOPA. According to the literature, three
421 TBDTs have been identified to be involved in the uptake of ferric-loaded catechol
422 siderophores: PfeA and PirA for enterobactin-Fe and protochelin-Fe and FvbA for
423 vibriobactin-Fe (Poole *et al.*, 1990; Ghysels *et al.*, 2005; Elias *et al.*, 2011; Gasser *et al.*, 2016),
424 these compounds all being tris-catechols. The mode of iron chelation by epinephrine,
425 norepinephrine, dopamine, and L-DOPA, as well as enterobactin and vibriobactin, involves
426 catechol functions. However, catecholamines are based on a 3,4-dihydroxyphenyl backbone,

whereas enterobactin and vibriobactin are based on a 2,3-dihydroxyphenyl backbone, implying steric hindrance that could explain the lack of interaction with PfeA. In addition, enterobactin (and most catechol-type siderophores) presents a carboxyl in alpha of the catechol cycle, thus leaving the possibility of a change in iron coordination between a catecholate mode and a salicylate mode (Abergel *et al.*, 2006), which may be important for the interaction with the PfeA transporter *in vivo*. In addition, importantly, the stoichiometry of iron chelation by catecholamines theoretically involves three catecholamines for a ferric ion. However, in solution, the existence of a mixture between complexes with stoichiometries of 3:1 (catecholamine:Fe^{3+}), 2:1, or even 1:1 with a molecule of water, citrate, or any other small molecule to complete the coordination cannot be excluded, as previously described for ferric complexes of pyochelin and citrate (Cobessi *et al.*, 2005; Mislin *et al.*, 2006; Silva *et al.*, 2009). Concerning enterobactin, only one form of ferric-enterobactin is formed, which is recognized by PfeA and, to a lesser extent, PirA. For the catecholamines, the existence of a mixture of ferric complexes with different chelation stoichiometries must have a certain impact on their recognition by the involved TBDTs and could explain why two different TBDTs, PirA and PiuA, with different binding selectivity, are involved in iron acquisition by these molecules. Moreover, the ^{55}Fe uptake assay used in this study was unable to show the involvement of PirA or PiuA in iron assimilation by catecholamines, whereas the growth assay with the Δ*pvdF*Δ*pchA* strain and its corresponding TBDT mutants was able to do so. Clearly, the sensitivity of the two assays is not the same for various reasons. The ^{55}Fe uptake assay lasted only 3 h, with cells in the stationary phase of growth, whereas the growth assay lasted 24 hours, with the cells being first in the exponential phase and then stationary phase of growth. Moreover, the concentration of iron and catecholamines was not the same in the two assays. The ^{55}Fe

uptake assay required a ^{55}Fe concentration of 500 nM to detect iron accumulation in bacteria and, consequently, a catecholamine concentration of 200 µM to avoid ^{55}Fe precipitation, which generates a high background of radioactive noise. In the growth assay, the iron concentration was approximately 20 nM (Cunrath *et al.*, 2016) and that of the catecholamines 10 µM. These assays certainly involve complexes with different iron:catechol stoichiometries, which can also explain the different results obtained for these two assays. It would also be informative to investigate the effects of catecholamine degradation products (oxidation of catecholamines). Indeed, aminochrome and adrenochrome, oxidation products of epinephrine and dopamine, as well as dihydroxyindole, may also play a role in iron uptake, as the catechol group, involved in iron chelation, is still present in these molecules and probably more of these molecules are formed during the 48-h culture assay than in the 3 h of ^{55}Fe uptake monitoring.

Despite these encouraging results, the molecular mechanisms involved in iron acquisition by catecholamines are far from being elucidated. There are likely a large number of proteins involved that have not been identified, such as inner-membrane transporters, and proteins involved in iron release from catecholamines. Nothing is currently known about the mechanism of iron release from the siderophores transported by the PirA and PiuA TBDTs. No genes encoding for an iron reductase or an inner membrane transporter are found next to *piA* and *pirA* on *P. aeruginosa* chromosome (Winsor *et al.*, 2016).

Moreover, the present study was carried out under *in vitro* conditions using planktonic cultures of *P. aeruginosa* to identify TBDTs involved in this uptake. Now that the TBDTs have been identified, it would be informative to determine what happens in an animal model that simulates a chronic *P. aeruginosa* infection. Moreover, the iron-reducing properties of

475 catecholamines need to be explored further, particularly for bacteria living in biofilms, a life
476 form in which ferrous iron has a more preponderant role than in planktonic cultures. Finally,
477 although catecholamines are unlikely to significantly compete with *P. aeruginosa*
478 siderophores, this does not exclude an important biological role for these molecules under
479 certain conditions, especially during chronic *P. aeruginosa* infections, for which it is known
480 that spontaneous mutations of the PvdS regulator can cause the absence of pyoverdine
481 secretion without, however, affecting the fitness of the bacteria. Such *pvdS* mutants may use
482 catecholamines as siderophores.
483
484 Although the study of the interactions between host catecholamines and pathogens is only
485 in its early stages, our data represent a major breakthrough by showing that dopamine, L-
486 DOPA, epinephrine, and norepinephrine are able to chelate iron and transport it efficiently
487 into *P. aeruginosa* cells via active proton-motive force-dependent uptake. The TBDTs
488 involved are PiuA and PirA, with the two transporters showing different uptake selectivity:
489 PiuA is more specific to dopamine and PirA appears to be more specific to L-DOPA and
490 norepinephrine. Ferrous iron uptake was also observed via the FeoABC system in the
491 presence of L-DOPA (Figure 7). How ferrous iron is transported across the outer membrane
492 stays unknown and probably occurs via porins. A possible candidate could be the homolog of
493 OprG of *Acinetobacter baumani* (Catel-Ferreira *et al.*, 2016; Chevalier *et al.*, 2017).
494

Material and Methods

Chemicals. Dopamine HCl, L-norepinephrine HCl, L-epinephrine bitartrate, L-DOPA, DL-normetanephrine HCl, enterobactin and protonophore CCCP (carbonyl cyanide *m*-chlorophenylhydrazone) were purchase from Sigma-Aldrich. PVD was purified as previously described (Demange *et al.*, 1990). Catecholamines and normetanephrine were solubilized at 100 mM in ultrapure water before use, with the exception of L-DOPA which was solubilized at 10 mM owing to its poor solubility in aqueous solution. $^{55}FeCl_3$ was obtained from Perkin Elmer Life and Analytical Sciences (Billerica, MA, USA).

Growth condition. The strains used are listed in Table SM1 in Supplementary Materials. *P. aeruginosa* was routinely precultured in LB medium for 24 h at 30°C with 220 rpm agitation before being transferred in iron-restricted CAA medium (casamino acid medium, composition: 5 g l^{-1} low-iron CAA (Difco), 1.46 g l^{-1} K_2HPO_4 $3H_2O$, 0.25 g l^{-1} $MgSO_4$ $7H_2O$) and incubated overnight at 30°C. Iron concentration in CAA medium is about 20 nM (Cunrath *et al.*, 2016).

Plasmid and Strain Construction. Enzymes were obtained from ThermoFisher Scientific. *Escherichia coli* strains SM10 or TOP10 (Invitrogen) were used as the host strains for the plasmids. Phusion High-Fidelity DNA polymerase (ThermoFisher Scientific) was used in order to amplify fragments from a preparation of *P. aeruginosa* PAO1 DNA. Primers are listed in Table 3SM. A 1400 bp insert containing the 700 bp flanking sequences of the gene and the HindIII, EcoRI or XhoI restriction sites was amplified for the construction of the pEXG2 Δ*PA0434,* pEXG2 Δ*piuA* and pEXG2 Δ*fvbA* plasmids. Both insert and empty pEXG2 plasmid were digested with appropriate restriction enzymes and inserts were subsequently cloned

520 into pEXG2 using cohesive end ligation with T4 DNA ligase. Mutations in the chromosomal
521 genome of *P. aeruginosa* were generated as previously described, by sequentially
522 introducing pEXG2 vectors using mating into *P. aeruginosa* PAO1 Δ*pvdF*Δ*pchA* and selecting
523 for deletion mutants before verification by PCR (polymerase chain reaction) and sequencing
524 (Perraud *et al.*, 2018).
525
526 ***Iron chelation assays.*** The CAS (Chrome Azurol S, purchased from Sigma) solution was
527 prepared according to Schwyn & Neilands as previously described (Perraud *et al.*, 2020)
528 with the omission of sulfocalicylic acid. 100 µL of the CAS-shuttle reagent at 7.5 µM was
529 incubated at room temperature in the presence of increasing concentrations of
530 catecholamines or normetanephrine for 1 h. For each concentration of compound tested,
531 the absorbance at 630 nm was monitored in a TECAN Infinite M200 plate reader.
532
533 ***Iron scavenging from pyoverdine-Fe.*** Pyoverdine was prepared in solution at 10 mM water
534 and the catecholamines as described above. The competition assay with pyoverdine-Fe was
535 carried out as described previously (Perraud *et al.*, 2020). PVD-Fe is prepared in solution at
536 10 µM in 100 µL of 100 mM HEPES buffer pH 7.4, and incubated at 25 °C in the presence of
537 increasing concentrations of catecholamines for 48 h. The fluorescence at 447 nm
538 corresponding to formed apo pyoverdine was monitored (excitation at 400 nm) in a TECAN
539 Infinite M200 plate reader.
540
541 ***Iron reduction assay.*** Iron(III) reduction in presence of catecholamines was monitored using
542 ferrozine (Sigma), a specific Fe^{2+} chelator. Ferrozine forms a stable magenta-colored solution
543 with Fe^{2+} and is therefore used as a reagent and indicator for Fe^{2+}. The complex has an

absorption peak at 562 nm. A mix of 0.5 mM of ferrozine and 50 µM of catecholamine in 100 mM HEPES buffer (pH 7.4) was added to a 96-well flat plate (Greiner). Right before the start of the experience, 50 µM of $FeCl_3$ in HCl 0.1 N were added to the wells and the increase of absorbance at 562 nm, corresponding to the formation of ferrozine-Fe(II) complex, was monitored using a TECAN M200 microplate reader. The positive control was performed using 100 mM of the reducing agent dithiothreitol instead of catecholamine.

^{55}Fe uptake assays. The iron uptake assays were carried out as previously described (Gasser *et al.*, 2016) except that the catecholamine-^{55}Fe complexes were prepared with a ratio of 400:1 (chelator: ^{55}Fe) and for enterobactin-^{55}Fe of 20:1 incubated for 15 minutes, catecholamines having a much lower affinity for iron compared to enterobactin and they chelate ferric iron with 3:1 stoichiometry. Concerning bacterial strains used, overnight cultures of *bacteria* cultivated in CAA medium were resuspended in 50 mM TrisHCl pH 8.0 buffer at an $OD_{600\ nm}$ of 1 and incubated with ^{55}Fe-catecholamine complexes at a final concentration of 500 nM for 3 h at 30°C. Aliquots were removed at different time, the bacteria pellet and radioactivity measured by scintillation counting.

Label-free proteomics analysis. *P. aeruginosa* PAO1 cells grown in CAA medium were diluted to an OD_{600nm} of 0.1 units and incubated in the absence or presence of 10 µM dopamine, L-DOPA, epinephrine, norepinephrine or normetanephrine at 30°C for 8 h. 5.10^8 cells from each culture were used for proteomic analysis. Each sample was prepared in biological triplicate for each cell culture condition. Cell pellets were resuspended in 200 µL of lysis buffer (UTCT buffer containing 7M urea, 2M thiourea, 4% CHAPS (3-[(3-cholamidopropyl)dimethylammonio]-1-propanesulfonate) and 20 mM Tris-HCl pH 7.6)

supplemented with nuclease and DNase. Protein concentrations were determined by Bradford assay using bovine serum albumin as standard. Proteins were further precipitated overnight with glacial 0.1 M ammonium acetate in 100 % methanol (5 volumes, -20°C). After centrifugation at 12.000 g and 4°C during 15 min, the resulting pellets were washed twice with 0.1 M ammonium acetate in 80% methanol and further dried under vacuum (Speed-Vac concentrator). Pellets were resuspended in 100 µL of 50 mM ammonium bicarbonate and submitted to reduction (5 mM Dithiothreitol, 95°C, 10 min) and alkylation (10 mM Iodoacetamide, room temperature, 20 min). Proteins were finally digested overnight with 150 ng of sequencing-grade trypsin (Promega). The proteomic datasets were obtained by the injection of 5000 ng of each peptidic mixture on a Q-Exactive Plus mass spectrometer coupled to an EASY-nanoLC-1000 (Thermo-Fisher Scientific, USA) as described previously (Perraud *et al.*, 2020).

The raw data obtained were converted into .mgf files with Proteome Discoverer Daemon software (Thermo-Fisher Scientific, script "Export-to-mgf", version 2.2). For both differential proteomic analyses, data were searched against the *P. aeruginosa* UniprotKB sub-database with a decoy strategy (UniprotKB release 2016_12, taxon 208964, *P. aeruginosa* strain PAO1, 5564 forward protein sequences). Peptides and proteins were identified with Mascot algorithm (version 2.5.1, Matrix Science, London, UK). The following parameters were used: (i) Trypsin/P was selected as enzyme, (ii) two missed cleavages were allowed, (iii) methionine oxidation and acetylation of protein N-term were set as variable modifications and carbamidomethylation of cysteine as fixed modification, (iv) mass tolerance for precursor ions was set at 10 ppm, and at 0.02 Da for fragment ions. Mascot data were further imported into Proline v1.4 software (http://proline.profiproteomics.fr/) (Bouyssié *et al.*, 2020). Proteins were validated on Mascot pretty rank equal to 1, and 1% FDR (False Discovery Rate) on both peptide spectrum matches (PSM score) and protein sets (Protein Set score). The total number

of MS/MS fragmentation spectra was used to quantify each protein from at least three independent biological replicates: this "BasicSC" value calculated by Proline includes all PSMs of all peptides, including the modified peptides (3 fixed and variable modifications) and the peptides shared by different protein sets. After a normalization of the data matrix with the total number of spectra in one sample, the "BasicSC" spectral count values were submitted to a negative-binomial test using an edgeR GLM regression through R (R v3.2.5). The statistical test was based on the published msmsTests R package available in Bioconductor to process label-free LC-MS/MS data by spectral counts (Gregori *et al.*, 2019). For each identified protein, an adjusted P-value (adjp) corrected by Benjamini–Hochberg was calculated, as well as a protein fold-change (FC).

Quantitative real-time PCR (qRT-PCR) on bacteria grown liquid culture. qRT-PCR was used to follow specific gene transcription as previously described (Gross and Loper, 2009; Gasser *et al.*, 2016). Bacteria were grown as for the proteomic analyses for 8 h, at 30°C, in the presence or absence of 10 µM dopamine, L-DOPA, epinephrine, norepinephrine or normetanephrine and with vigorous shaking. An aliquot of 2.5 x 10^8 cells from this culture was added to two volumes of RNAprotect Bacteria Reagent (Qiagen) and exactly the same protocol was used as previously described (Perraud *et al.*, 2020). Primer efficiency were determined using serially diluted genomic DNA and the double ΔC_T method was used to analyze qPCR data.

Growth screening in the absence and presence of catecholamines of different P. aeruginosa TBDT mutants. Overnight cultures of *P. aeruginosa,* grown in CAA medium, were seeded at an $OD_{600\ nm}$ of 0.02 in 200 µL fresh CAA medium in the absence or presence of

617 norepinephrine, epinephrine, dopamine, L-DOPA or normetanephrine, in 96 well U-shaped
618 plates (Greiner). Fresh, sterile-filtered aqueous solutions of the tested compounds were
619 added at a final concentration of 10 µM. $OD_{600\ nm}$ was monitored in an Infinite M200 (TECAN,
620 Austria) plate reader for 22 h, with regular agitation and incubation temperature set to 30°C.
621 Growth rescue assays in presence of enterobactin were performed following the same
622 procedure, with enterobactin being dissolved at 10 mM in dimethylsulfoxide and added at a
623 final concentration of 10 µM.
624
625
626
627 **ACKNOWLEDGMENTS**
628 This work was partially funded by the *Centre National de la Recherche Scientifique* and
629 grants from the association Vaincre la Mucoviscidose and Association Gregory Lemarchal.
630 The mass spectrometry instrumentation at the IBMC was funded by the University of
631 Strasbourg, IdEx "Equipement mi-lourd" 2015. QP had a fellowship from the association
632 Vaincre la Mucoviscidose and Association Gregory Lemarchal.
633

635 **References**

636 Abergel, R.J., Warner, J.A., Shuh, D.K., and Raymond, K.N. (2006) Enterobactin protonation
637 and iron release: structural characterization of the salicylate coordination shift in ferric
638 enterobactin. *J Am Chem Soc* **128**: 8920–8931.

639 Albrecht-Gary, A.M., Blanc, S., Rochel, N., Ocacktan, A.Z., and Abdallah, M.A. (1994) Bacterial
640 iron transport: coordination properties of pyoverdin PaA, a peptidic siderophore of
641 *Pseudomonas aeruginosa*. *Inorg Chem* **33**: 6391–6402.

642 Anderson, M.T., and Armstrong, S.K. (2008) Norepinephrine mediates acquisition of
643 transferrin-iron in *Bordetella bronchiseptica*. *J Bacteriol* **190**: 3940–3947.

644 Belkaid, Y., and Hand, T.W. (2014) Role of the Microbiota in Immunity and Inflammation. *Cell*
645 **157**: 121–141.

646 Bluhm, M.E., Kim, S.S., Dertz, E.A., and Raymond, K.N. (2002) Corynebactin and
647 enterobactin: related siderophores of opposite chirality. *J Am Chem Soc* **124**: 2436–2437.

648 Bouyssié, D., Hesse, A.-M., Mouton-Barbosa, E., Rompais, M., Macron, C., Carapito, C., *et al.*
649 (2020) Proline: an efficient and user-friendly software suite for large-scale proteomics.
650 *Bioinformatics* **36**: 3148–3155.

651 Brandel, J., Humbert, N., Elhabiri, M., Schalk, I.J., Mislin, G.L.A., and Albrecht-Garry, A.-M.
652 (2012) Pyochelin, a siderophore of *Pseudomonas aeruginosa*: Physicochemical
653 characterization of the iron(III), copper(II) and zinc(II) complexes. *Dalton Trans* **41**: 2820–34.

654 Burton, C.L., Chhabra, S.R., Swift, S., Baldwin, T.J., Withers, H., Hill, S.J., and Williams, P.
655 (2002) The growth response of *Escherichia coli* to neurotransmitters and related
656 catecholamine drugs requires a functional enterobactin biosynthesis and uptake system.
657 *Infect Immun* **70**: 5913–5923.

658 Catel-Ferreira, M., Marti, S., Guillon, L., Jara, L., Coadou, G., Molle, V., *et al.* (2016) The outer

membrane porin OmpW of *Acinetobacter baumannii* is involved in iron uptake and colistin binding. *FEBS Let* **590**: 224–231.

Chevalier, S., Bouffartigues, E., Bodilis, J., Maillot, O., Lesouhaitier, O., Feuilloley, M.G.J., *et al.* (2017) Structure, function and regulation of *Pseudomonas aeruginosa* porins. *FEMS Microbiol Rev* **41**: 698–722.

Clément, E., Mesini, P.J., Pattus, F., Abdallah, M.A., and Schalk, I.J. (2004) The binding mechanism of pyoverdin with the outer membrane receptor FpvA in *Pseudomonas aeruginosa* is dependent on its iron-loaded status. *Biochemistry* **43**: 7954–65.

Cobessi, D., Celia, H., and Pattus, F. (2005) Crystal structure at high resolution of ferric-pyochelin and its membrane receptor FptA from *Pseudomonas aeruginosa*. *J Mol Biol* **352**: 893–904.

Cooper, E.V. (1946) Gas-gangrene following injection of adrenaline. *Lancet* **1**: 459–461.

Cornelis, P., and Dingemans, J. (2013) *Pseudomonas aeruginosa* adapts its iron uptake strategies in function of the type of infections. *Front Cell Infect Microbiol* **3**: 75.

Cornish, A.S., and Page, W.J. (2000) Role of molybdate and other transition metals in the accumulation of protochelin by *Azotobacter vinelandii*. *Appl Environ Microbiol* **66**: 1580–6.

Cunrath, O., Geoffroy, V.A., and Schalk, I.J. (2016) Metallome of *Pseudomonas aeruginosa*: a role for siderophores. *Environ Microbiol* **18**: 3258–3267.

Damron, F.H., Oglesby-Sherrouse, A.G., Wilks, A., and Barbier, M. (2016) Dual-seq transcriptomics reveals the battle for iron during *Pseudomonas aeruginosa* acute murine pneumonia. *Sci Rep* **6**: 39172.

Dean, C.R., Neshat, S., and Poole, K. (1996) PfeR, an enterobactin-responsive activator of ferric enterobactin receptor gene expression in *Pseudomonas aeruginosa*. *J Bacteriol* **178**: 5361–5369.

683 Dean, C.R., and Poole, K. (1993) Cloning and characterization of the ferric enterobactin
684 receptor gene (*pfeA*) of *Pseudomonas aeruginosa*. *J Bacteriol* **175**: 317–324.
685 Demange, P., Wendenbaum, S., Linget, C., Mertz, C., Cung, M.T., and Dell, A., Abdallah, M.A.
686 (1990) Bacterial siderophores: structure and NMR assigment of pyoverdins PaA,
687 siderophores of *Pseudomonas aeruginosa* ATCC 15692. *Biol Metals* **3**: 155–170.
688 Dichtl, S., Demetz, E., Haschka, D., Tymoszuk, P., Petzer, V., Nairz, M., *et al.* (2019) Dopamine
689 is a siderophore-like iron chelator that promotes *Salmonella enterica* serovar Typhimurium
690 virulence in mice. *mBio* **10**.
691 Doring, G., Pfestorf, M., Botzenhart, K., and Abdallah, M.A. (1988) Impact of proteases on
692 iron uptake of *Pseudomonas aeruginosa* pyoverdin from transferrin and lactoferrin. *Infect*
693 *Immun* **56**: 291–3.
694 Eisenhofer, G., Kopin, I.J., and Goldstein, D.S. (2004) Catecholamine metabolism: a
695 contemporary view with implications for physiology and medicine. *Pharmacol Rev* **56**: 331–
696 349.
697 Elias, S., Degtyar, E., and Banin, E. (2011) FvbA is required for vibriobactin utilization in
698 *Pseudomonas aeruginosa*. *Microbiology* **157**: 2172–80.
699 Evans, D.G., Miles, A.A., and Niven, J.S.F. (1948) The enhancement of bacterial infections by
700 adrenaline. *Br J Exp Pathol* **29**: 20–39.
701 Folschweiller, N., Gallay, J., Vincent, M., Abdallah, M.A., Pattus, F., and Schalk, I.J. (2002) The
702 interaction between pyoverdin and its outer membrane receptor in *Pseudomonas*
703 *aeruginosa* leads to different conformers: a time-resolved fluorescence study. *Biochemistry*
704 **41**: 14591–601.
705 Freestone, P.P., Haigh, R.D., Williams, P.H., and Lyte, M. (2003) Involvement of enterobactin
706 in norepinephrine-mediated iron supply from transferrin to enterohaemorrhagic *Escherichia*

coli. *FEMS Microbiol Lett* **222**: 39–43.

Galet, J., Deveau, A., Hôtel, L., Frey-Klett, P., Leblond, P., and Aigle, B. (2015) *Pseudomonas fluorescens* pirates both ferrioxamine and ferricoelichelin siderophores from *Streptomyces ambofaciens*. *Appl Environ Microbiol* **81**: 3132–3141.

Gasser, V., Baco, E., Cunrath, O., August, P.S., Perraud, Q., Zill, N., *et al.* (2016) Catechol siderophores repress the pyochelin pathway and activate the enterobactin pathway in *Pseudomonas aeruginosa*: an opportunity for siderophore-antibiotic conjugates development. *Environ Microbiol* **18**: 819–832.

Ghysels, B., Dieu, B.T., Beatson, S.A., Pirnay, J.P., Ochsner, U.A., Vasil, M.L., and Cornelis, P. (2004) FpvB, an alternative type I ferripyoverdine receptor of *Pseudomonas aeruginosa*. *Microbiology* **150**: 1671–80.

Ghysels, B., Ochsner, U., Mollman, U., Heinisch, L., Vasil, M., Cornelis, P., and Matthijs, S. (2005) The *Pseudomonas aeruginosa pirA* gene encodes a second receptor for ferrienterobactin and synthetic catecholate analogues. *FEMS Microbiol Lett* **246**: 167–74.

Gregori, J., Sanchez, A., and Villanueva, J. (2019) *msmsTests: LC-MS/MS Differential Expression Tests*. Bioconductor version: Release (3.9), . https://bioconductor.org/packages/msmsTests/. Accessed October 25, 2019.

Gross, H., and Loper, J.E. (2009) Genomics of secondary metabolite production by *Pseudomonas* spp. *Nat Prod Rep* **26**: 1408–46.

Groves, A.C., Griffiths, J., Leung, F., and Meek, R.N. (1973) Plasma catecholamines in patients with serious postoperative infection. *Ann Surg* **178**: 102–107.

Harris, W.R., Carrano, C.J., Cooper, S.R., Sofen, S.R., Avdeef, A.E., McArdle, J.V., and Raymond, K.N. (1979) Coordination chemistry of microbial iron transport compounds. 19. Stability constants and electrochemical behavior of ferric enterobactin and model

731 complexes. *J Am Chem Soc* **101**: 6097–6104.

732 Hegde, M., Wood, T.K., and Jayaraman, A. (2009) The neuroendocrine hormone
733 norepinephrine increases *Pseudomonas aeruginosa* PA14 virulence through the las quorum-
734 sensing pathway. *Appl Microbiol Biotechnol* **84**: 763–776.

735 Hider, R.C., and Kong, X. (2011) Chemistry and biology of siderophores. *Nat Prod Rep* **27**:
736 637–57.

737 Hughes, D.T., Clarke, M.B., Yamamoto, K., Rasko, D.A., and Sperandio, V. (2009) The QseC
738 adrenergic signaling cascade in *Enterohemorrhagic E. coli* (EHEC). *PLoS Pathog* **5**: e1000553.

739 Jones, S.B., Westfall, M.V., and Sayeed, M.M. (1988) Plasma catecholamines during *E. coli*
740 bacteremia in conscious rats. *Am J Physiol* **254**: R470-477.

741 Liu, X., Yamada, N., Maruyama, W., and Osawa, T. (2008) Formation of dopamine adducts
742 derived from brain polyunsaturated fatty acids. *J Biol Chem* **283**: 34887–34895.

743 Llamas, M.A., Imperi, F., Visca, P., and Lamont, I.L. (2014) Cell-surface signaling in
744 *Pseudomonas*: stress responses, iron transport, and pathogenicity. *FEMS Microbiol Rev* **38**:
745 569–97.

746 Llamas, M.A., Mooij, M.J., Sparrius, M., Vandenbroucke-Grauls, C.M., Ratledge, C., and
747 Bitter, W. (2008) Characterization of five novel *Pseudomonas aeruginosa* cell-surface
748 signaling systems. *Mol Microbiol* **67**: 458–72.

749 Llamas, M.A., Sparrius, M., Kloet, R., Jimenez, C.R., Vandenbroucke-Grauls, C., and Bitter, W.
750 (2006) The heterologous siderophores ferrioxamine B and ferrichrome activate signaling
751 pathways in *Pseudomonas aeruginosa*. *J Bacteriol* **188**: 1882–91.

752 May, J.J., Wendrich, T.M., and Marahiel, M.A. (2001) The dhb operon of Bacillus subtilis
753 encodes the biosynthetic template for the catecholic siderophore 2,3-dihydroxybenzoate-
754 glycine-threonine trimeric ester bacillibactin. *J Biol Chem* **276**: 7209–7217.

Melin, V., Henríquez, A., Freer, J., and Contreras, D. (2015) Reactivity of catecholamine-driven Fenton reaction and its relationships with iron(III) speciation. *Redox Rep* **20**: 89–96.

Meyer, J.M., Neely, A., Stintzi, A., Georges, C., and Holder, I.A. (1996) Pyoverdin is essential for virulence of *Pseudomonas aeruginosa*. *Infect Immun* **64**: 518–23.

Miethke, M., and Skerra, A. (2010) Neutrophil gelatinase-associated lipocalin expresses antimicrobial activity by interfering with L-norepinephrine-mediated bacterial iron acquisition. *Antimicrob Agents Chemother* **54**: 1580–1589.

Mislin, G.L.A., Hoegy, F., Cobessi, D., Poole, K., Rognan, D., and Schalk, I.J. (2006) Binding properties of pyochelin and structurally related molecules to FptA of *Pseudomonas aeruginosa*. *J Mol Biol* **357**: 1437–48.

Moynié, L., Luscher, A., Rolo, D., Pletzer, D., Tortajada, A., Weingart, H., *et al.* (2017) Structure and Function of the PiuA and PirA Siderophore-Drug Receptors from *Pseudomonas aeruginosa* and *Acinetobacter baumannii*. *Antimicrob Agents Chemother* **61**(4):e02531-16.

Müller, S.I., Valdebenito, M., and Hantke, K. (2009) Salmochelin, the long-overlooked catecholate siderophore of *Salmonella*. *Biometals* **22**: 691–695.

Normant, V.P., Josts, I., Kuhn, L., Perraud, Q., Fritsch, S., Hammann, P., *et al.* (2020) Nocardamine-dependent iron uptake in *Pseudomonas aeruginosa*: exclusive involvement of the FoxA outer membrane transporter. *ACS Chem Biol* 15: 2741-2751.

O'Brien, I.G., and Gibson, F. (1970) The structure of enterochelin and related 2,3-dihydroxy-N-benzoylserine conjugates from *Escherichia coli*. *Biochim Biophys Acta* **215**: 393–402.

Perraud, Q., Cantero, P., Roche, B., Gasser, V., Normant, V.P., Kuhn, L., *et al.* (2020) Phenotypic adaption of *Pseudomonas aeruginosa* by hacking siderophores produced by other microorganisms. *Mol Cell Proteomics* **19**: 589–607.

Perraud, Q., Moynié, L., Gasser, V., Munier, M., Godet, J., Hoegy, F., *et al.* (2018) A key role

779 for the periplasmic PfeE esterase in iron acquisition via the siderophore enterobactin in
780 *Pseudomonas aeruginosa*. *ACS Chem Biol* **13**: 2603–2614.
781 Pollack, J.R., and Neilands, J.B. (1970) Enterobactin, an iron transport compound from
782 *Salmonella typhimurium*. *Biochem Biophys Res Commun* **38**: 989–992.
783 Poole, K., Young, L., and Neshat, S. (1990) Enterobactin-mediated iron transport in
784 *Pseudomonas aeruginosa*. *J Bacteriol* **172**: 6991–6.
785 Raymond, K.N., Dertz, E.A., and Kim, S.S. (2003) Enterobactin: an archetype for microbial
786 iron transport. *Proc Natl Acad Sci USA* **100**: 3584–8.
787 Reading, N.C., Rasko, D.A., Torres, A.G., and Sperandio, V. (2009) The two-component
788 system QseEF and the membrane protein QseG link adrenergic and stress sensing to
789 bacterial pathogenesis. *Proc Natl Acad Sci USA* **106**: 5889–5894.
790 Roshchina, V.V. (2016) New trends and perspectives in the evolution of neurotransmitters in
791 microbial, plant, and animal cells. *Adv Exp Med Biol* **874**: 25–77.
792 Sandrini, S.M., Shergill, R., Woodward, J., Muralikuttan, R., Haigh, R.D., Lyte, M., and
793 Freestone, P.P. (2010) Elucidation of the mechanism by which catecholamine stress
794 hormones liberate iron from the innate immune defense proteins transferrin and lactoferrin.
795 *J Bacteriol* **192**: 587–594.
796 Schalk, I.J., Abdallah, M.A., and Pattus, F. (2002) Recycling of pyoverdin on the FpvA receptor
797 after ferric pyoverdin uptake and dissociation in *Pseudomonas aeruginosa*. *Biochemistry* **41**:
798 1663–1671.
799 Schalk, I.J., and Guillon, L. (2013) Fate of ferrisiderophores after import across bacterial
800 outer membranes: different iron release strategies are observed in the cytoplasm or
801 periplasm depending on the siderophore pathways. *Amino Acids* **44**: 1267–1277.
802 Schalk, I.J., Rigouin, C., and Godet, J. (2020) An overview of siderophore biosynthesis among

fluorescent Pseudomonads and new insights into their complex cellular organization. *Environ Microbiol* **22**: 1447–1466.

Schwyn, B., and Neilands, J.B. (1987) Universal chemical assay for the detection and determination of siderophores. *Anal Biochem* **160**: 47–56.

Silva, A.M., Kong, X., Parkin, M.C., Cammack, R., and Hider, R.C. (2009) Iron(III) citrate speciation in aqueous solution. *Dalton Trans* **40**: 8616–8625.

Siraki, A.G., Smythies, J., and O'Brien, P.J. (2000) Superoxide radical scavenging and attenuation of hypoxia-reoxygenation injury by neurotransmitter ferric complexes in isolated rat hepatocytes. *Neurosci Lett* **296**: 37–40.

Stookey, L.L. (1970) Ferrozine-A New Spectrophotometric Reagent for Iron. *Anal Chem* **42**: 779–781.

Traxler, M.F., Seyedsayamdost, M.R., Clardy, J., and Kolter, R. (2012) Interspecies modulation of bacterial development through iron competition and siderophore piracy. *Mol Microbiol* **86**: 628–44.

Verbrugghe, E., Boyen, F., Gaastra, W., Bekhuis, L., Leyman, B., Van Parys, A., *et al.* (2012) The complex interplay between stress and bacterial infections in animals. *Vet Microbiol* **155**: 115–127.

Winsor, G.L., Griffiths, E.J., Lo, R., Dhillon, B.K., Shay, J.A., and Brinkman, F.S.L. (2016) Enhanced annotations and features for comparing thousands of *Pseudomonas* genomes in the *Pseudomonas* genome database. *Nucleic Acids Res* **44**: D646-653.

Yoo, J.Y., Groer, M., Dutra, S.V.O., Sarkar, A., and McSkimming, D.I. (2020) Gut microbiota and immune system interactions. *Microorganisms* **8**.

Zhang, Y., Edmonds, K.A., Raines, D.J., Murphy, B.A., Wu, H., Guo, C., *et al.* (2020) The Pneumococcal iron uptake protein A (PiuA) specifically recognizes tetradentate FeIII-bis- and

827 mono-catechol complexes. *J Mol Biol* **432**: 5390–5410.

828

829

Figure legends

Figure 1. Structure of dopamine, L-DOPA, epinephrine, norepinephrine, and normetanephrine. Iron chelating groups are shown in red.

Figure 2. A. Ability of the various catecholamines to scavenge iron from CAS-Fe complexes. CAS-Fe 7.5 µM) was incubated with increasing concentrations of pyoverdine, pyochelin, dopamine, L-DOPA, epinephrine, norepinephrine, and normetanephrine, as described in Materials and Methods. CAS-Fe dissociation was followed by monitoring the absorbance at 630 nm. The data were normalized using $(A_{MEASURED} - A_{apoCAS})/(A_{apoCAS} - A_{CAS\text{-}Fe})$, $A_{MEASURED}$ for the absorbance measured for each experimental condition, A_{apoCAS} for the absorbance of CAS without iron, and $A_{CAS\text{-}Fe}$ for the absorbance of CAS loaded with iron.

B. Ability of the various catecholamines to scavenge iron from pyoverdine-Fe complexes. PVD-Fe (10 µM) in 100 mM HEPES pH 7.4 was incubated with increasing concentrations of TCV, dopamine, L-DOPA, epinephrine, norepinephrine, and normetanephrine, as described in Materials and Methods, for 48 h (until equilibrium was reached), as described previously (Perraud *et al.*, 2020). Metal-free PVD is fluorescent, with absorbance typically at 447 nm, and PVD-Fe is not (Albrecht-Gary *et al.*, 1994; Folschweiller *et al.*, 2002). Apo PVD formation was thus followed by monitoring fluorescent at 447 nm (excitation at 400 nm). The data were normalized using the formula $(F_{MEASURED} - F_{PVD\text{-}Fe})/(F_{PVD} - F_{PVD\text{-}Fe})$, $F_{MEASURED}$ being the fluorescence measured for each experimental condition, $F_{PVD\text{-}Fe}$ the fluorescence of 10 µM PVD-Fe, and F_{PVD} the fluorescence of 10 µM PVD.

C. Kinetics of iron reduction. $FeCl_3$ (50 µM) was incubated in 100 mM HEPES buffer at pH 7.4, in the presence of 0.5 mM ferrozine (gray line), 0.5 mM ferrozine and 100 mM DTT

(black line), or 0.5 mM ferrozine and 50 µM of each of the catecholamines (dopamine: blue line, L-DOPA: red, epinephrine: orange, norepinephrine: green, and normetanephrine: pink). The formation of ferrozine-Fe^{2+} was followed at 562 nm every 60 s. The graph on the right is a zoom of the graph on the left.

Figure 3. A. ^{55}Fe uptake by *ΔpvdFΔpchA* and *ΔpvdFΔpchAΔpfeAΔpirAΔpiuAΔfvbAΔPA0434* cells in the presence of the catecholamines. The strains were grown in CAA medium supplemented with one of the catecholamines (dopamine, L-D0PA, epinephrine, or norepinephrine) to activate the expression of the corresponding inducible uptake pathway. Then, bacteria were harvested and incubated in 50 mM Tris-HCl pH 8.0 in the presence of 500 nM ^{55}Fe in complex with catecholamines. Since catecholamines have a low affinity for iron relative to siderophores, they were mixed with ^{55}Fe in a 400:1 (catecholamines:^{55}Fe) ratio, as described in Materials and Methods (at a lower ratio, such as 20:1, a small amount of iron precipitation was observed, affecting the ^{55}Fe-uptake data). Aliquots were removed at various times, the bacteria pelleted, and the radioactivity retained in the cells measured. In each panel, uptake by Δ*pvdF*Δ*pchA* cells is shown in blue and that by Δ*pvdF*Δ*pchA*Δ*pfeA*Δ*pirA*Δ*piuA*Δ*fvbA*Δ*PA0434* cells in yellow. For each siderophore, the uptake assays with *ΔpvdFΔpchA* cells were also performed in the presence of the protonophore CCCP (green curve) to differentiate proton-motive force-dependent transport from diffusion or nonspecific interactions. For each curve, the data represent the mean of three independent experiments.

Figure 4. Analysis of changes in the expression of proteins involved in iron-uptake pathways in *P. aeruginosa cells* grown under iron-limited conditions (CAA medium) in the

879 **absence or presence of catecholamines. A.** Proteomic analyses were performed on the
880 pyoverdine- and pyochelin-deficient *P. aeruginosa* strains (Δ*pvdF*Δ*pchA*) grown overnight in
881 CAA supplemented, or not, with 10 µM dopamine, L-DOPA, epinephrine, norepinephrine, or
882 normetanephrine. Average values measured in CAA in the absence of any supplementation
883 with siderophores are plotted against average values measured in CAA supplemented with
884 either 10 µM catecholamines or normetanephrine. Median values represent the median of
885 the relative intensity of each protein, normalized against all proteins detected by shotgun
886 analysis (n = 3). The proteins of the pyochelin pathway are represented by yellow dots, those
887 of the pyoverdine pathway by green dots, and the TBDTs by blue dots. Sup Data 1 shows the
888 detailed results of protein identification and quantitation.
889 **B.** Heat maps of various TBDTs and proteins involved in the pyochelin and pyoverdine iron
890 uptake pathways: the darker the shade of blue, the higher the expression of the protein; the
891 darker the shade of red, the more the expression of the protein is repressed. Only the
892 proteins for which a change in the level of expression was observed are shown. FecA, FptA,
893 FpvA, PA0434, PA3268, PfeA, PhuR, and PirA are TBDTs; FpvA, FpvC, PvdI, PvdL, and PvdQ
894 are proteins of the pyoverdine-dependent iron-uptake pathway; FptA, PchB, PchC, PchD,
895 PchE, and PchF are proteins of the pyochelin-dependent iron-uptake pathway.
896
897 **Figure 5. Analysis of changes in the transcription of genes encoding TBDTs involved in iron-**
898 **uptake pathways in *P. aeruginosa cells* grown under iron-limited conditions (CAA medium)**
899 **in the absence or presence of catecholamines.** RT-qPCR was performed on pyoverdine- and
900 pyochelin-deficient *P. aeruginosa* strains (Δ*pvdF*Δ*pchA*) grown in CAA medium for 8 h, as
901 described in Materials and Methods, with or without 10 µM dopamine, L-DOPA,
902 epinephrine, norepinephrine, and normetanephrine. The data were normalized relative to

the reference gene *uvrD* and are representative of three independent experiments performed in triplicate (*n* = 3). Results are presented as the ratio between the values obtained in the presence of the catecholamines or normetanephrine over those obtained in their absence. *fecA* encodes the TBDT of ferri-citrate, *feoB* the ferrous inner membrane transporter, *fptA* and *fpvA* the TBDTs of pyochelin and pyoverdine, respectively, *pfeA and pirA* the TBDT of ENT, and piuA the TBDT of an unknown xenosiderophore.

Figure 6. Growth of different *P. aeruginosa* TBDT mutants in the absence or presence of 10 µM catecholamines. The strains used are a pyoverdine and pyochelin mutant (Δ*pvdF*Δ*pchA*) and its corresponding TBDT deletion mutants. Strains were grown in CAA medium in the absence (Ctrl for control, kinetics in black) or presence of 10 µM catecholamines or normetanephrine. Growth was followed by monitoring optical density (OD) at 600 nm.

Figure 7: Transporters involved in iron acquisition by catecholamines in *P. aeruginosa*. Catecholamines transport iron in *P. aeruginosa* cells via the TBDTs PirA and PiuA. Catecholamine-Fe complexes are able to induce *pirA* transcription probably by interacting in the bacterial periplasm with the sensor of the two-component system PfeS/PirR (PirA being the transcriptional regulator). In the presence of L-DOPA, ferrous uptake is observed involving the FeoABC system.

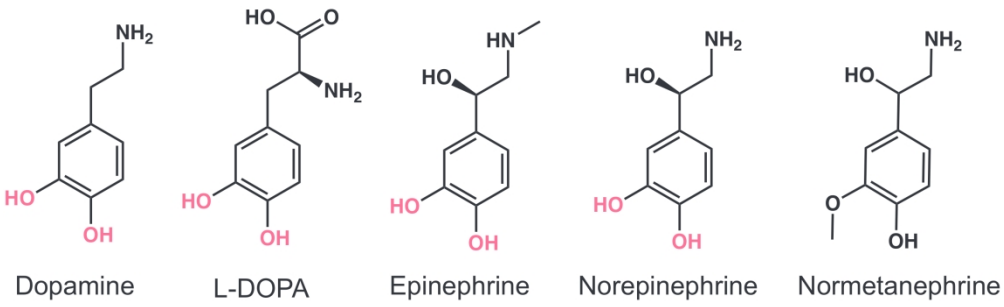

Figure 1. Structure of dopamine, L-DOPA, epinephrine, norepinephrine, and normetanephrine. Iron chelating groups are shown in red.

241x71mm (300 x 300 DPI)

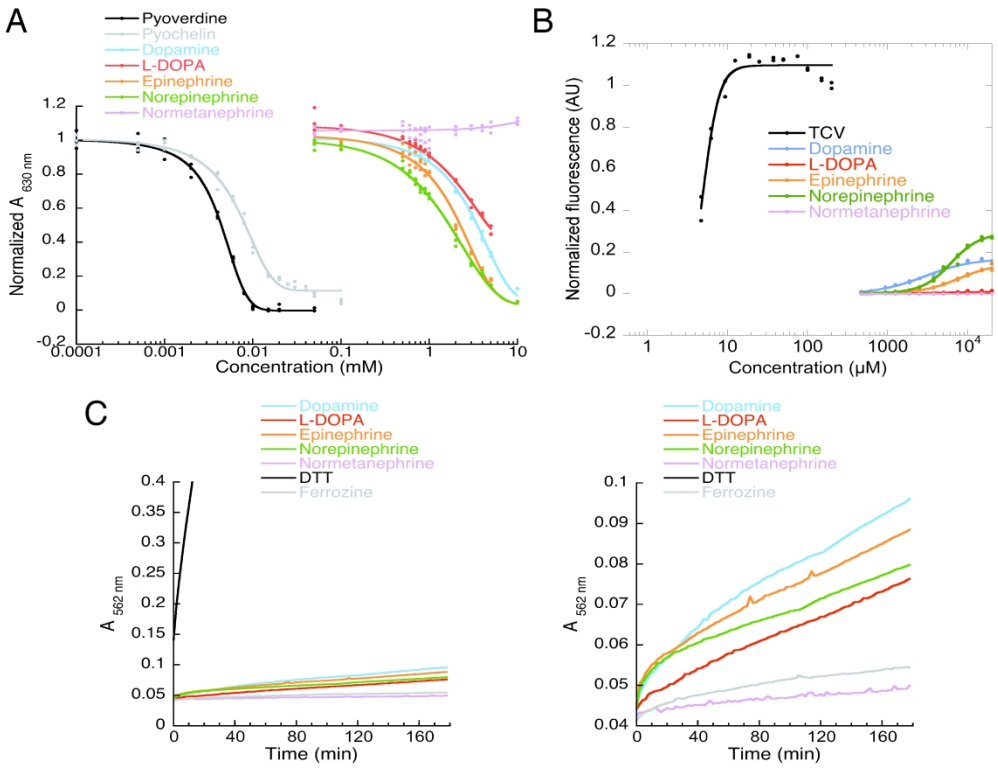

Figure 2. A. Ability of the various catecholamines to scavenge iron from CAS-Fe complexes. CAS-Fe 7.5 µM) was incubated with increasing concentrations of pyoverdine, pyochelin, dopamine, L-DOPA, epinephrine, norepinephrine, and normetanephrine, as described in Materials and Methods. CAS-Fe dissociation was followed by monitoring the absorbance at 630 nm. The data were normalized using $(A_{MEASURED} - A_{apoCAS})/(A_{apoCAS} - A_{CAS\text{-}Fe}$, $A_{MEASURED}$ for the absorbance measured for each experimental condition, A_{apoCAS} for the absorbance of CAS without iron, and $A_{CAS\text{-}Fe}$ for the absorbance of CAS loaded with iron. B. Ability of the various catecholamines to scavenge iron from PVD-Fe complexes. PVD-Fe (10 µM) in 100 mM HEPES pH 7.4 was incubated with increasing concentrations of TCV, dopamine, L-DOPA, epinephrine, norepinephrine, and normetanephrine, as described in Materials and Methods, for 48 h (until equilibrium was reached), as described previously (Perraud *et al.*, 2020b). Metal-free PVD is fluorescent, with absorbance typically at 447 nm, and PVD-Fe is not (Albrecht-Gary *et al.*, 1994; Folschweiller *et al.*, 2002). Apo PVD formation was thus followed by monitoring fluorescent at 447 nm (excitation at 400 nm). The data were normalized using the formula $(F_{MEASURED} - F_{PVD\text{-}Fe})/(F_{PVD} - F_{PVD\text{-}Fe})$, $F_{MEASURED}$ being the fluorescence measured for each experimental condition, $F_{PVD\text{-}Fe}$ the fluorescence of 10 µM PVD-Fe, and F_{PVD} the fluorescence of 10 µM PVD. C. Kinetics of iron reduction. $FeCl_3$ (50 µM) was incubated in 100 mM HEPES buffer at pH 7.4, in the presence of 0.5 mM ferrozine (gray line), 0.5 mM ferrozine and 100 mM DTT (black line), or 0.5 mM ferrozine and 50 µM of each of the catecholamines (dopamine: blue line, L-DOPA: red, epinephrine: orange, norepinephrine: green, and normetanephrine: pink). The formation of ferrozine-Fe2+ was followed at 562 nm every 60 s. The graph on the right is a zoom of the graph on the left.

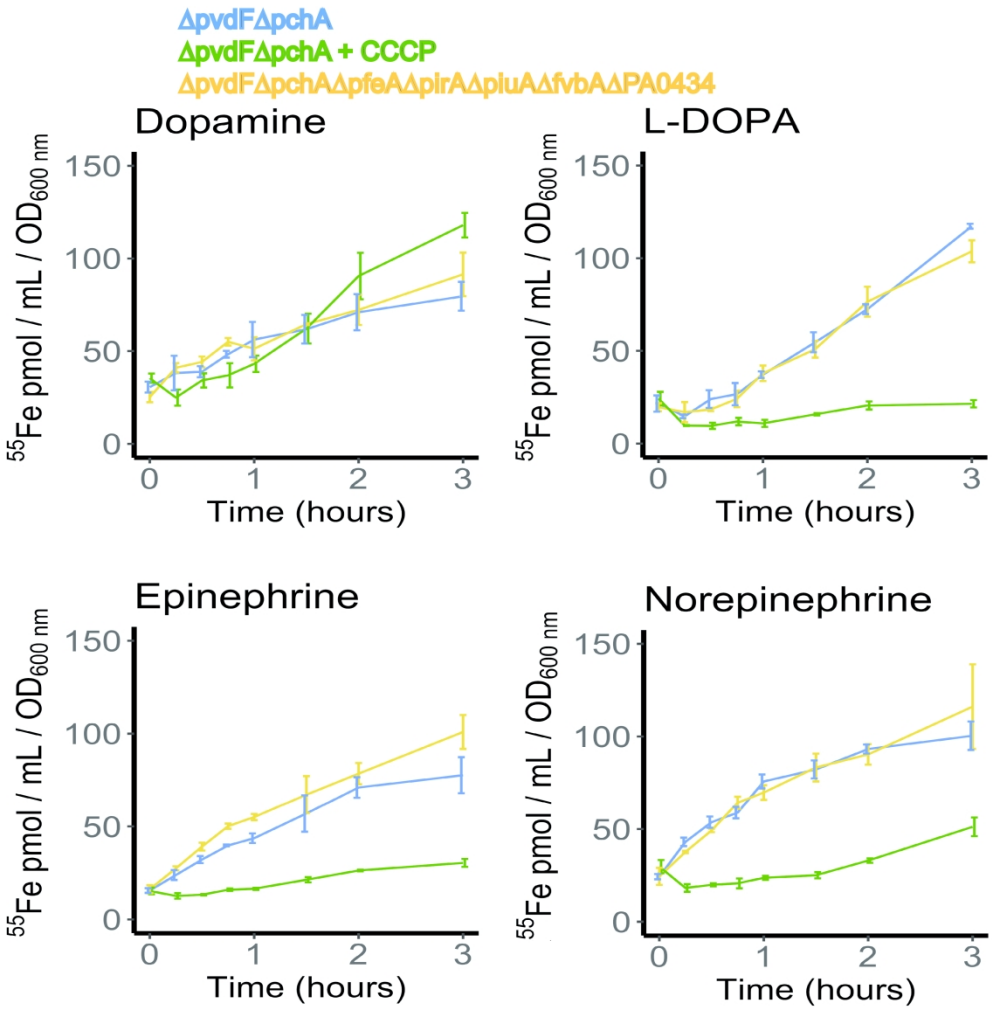

Figure 3. A. ^{55}Fe uptake by Δ*pvdF*Δ*pchA* and Δ*pvdF*Δ*pchA*Δ*pfeA*Δ*pirA*Δ*piuA*Δ*fvbA*Δ*PA0434* cells in the presence of the catecholamines. The strains were grown in CAA medium supplemented with one of the catecholamines (dopamine, L-D0PA, epinephrine, or norepinephrine) to activate the expression of the corresponding inducible uptake pathway. Then, bacteria were harvested and incubated in 50 mM Tris-HCl pH 8.0 in the presence of 500 nM ^{55}Fe in complex with catecholamines. Since catecholamines have a low affinity for iron relative to siderophores, they were mixed with ^{55}Fe in a 400:1 (catecholamines:^{55}Fe) ratio, as described in Materials and Methods (at a lower ratio, such as 20:1, a small amount of iron precipitation was observed, affecting the ^{55}Fe-uptake data). Aliquots were removed at various times, the bacteria pelleted, and the radioactivity retained in the cells measured. In each panel, uptake by Δ*pvdF*Δ*pchA* cells is shown in blue and that by Δ*pvdF*Δ*pchA*Δ*pfeA*Δ*pirA*Δ*piuA*Δ*fvbA*Δ*PA0434* cells in yellow. For each siderophore, the uptake assays with Δ*pvdF*Δ*pchA* cells were also performed in the presence of the protonophore CCCP (green curve) to differentiate proton-motive force-dependent transport from diffusion or nonspecific interactions. For each curve, the data represent the mean of three independent experiments.

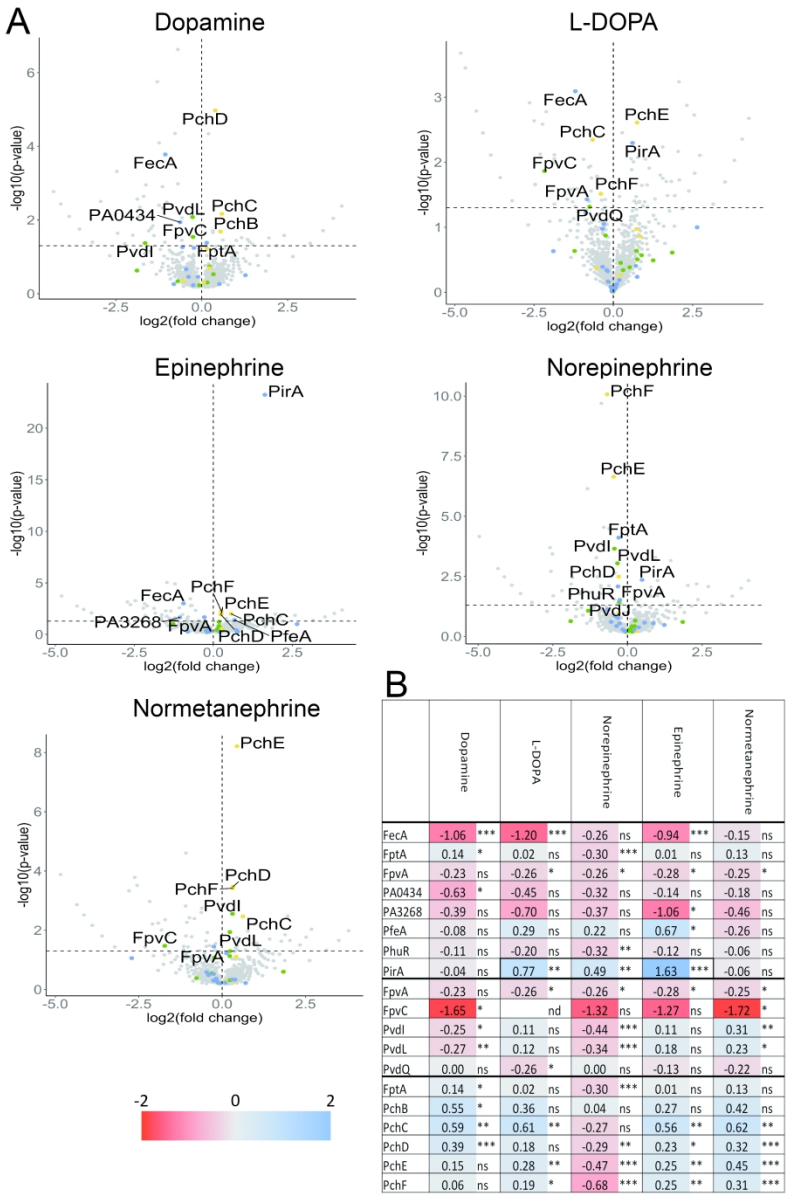

Figure 4. Analysis of changes in the expression of proteins involved in iron-uptake pathways in P. aeruginosa cells grown under iron-limited conditions (CAA medium) in the absence or presence of catecholamines. A. Proteomic analyses were performed on the pyoverdine- and pyochelin-deficient *P. aeruginosa* strains (Δ*pvdF*Δ*pchA*) grown overnight in CAA supplemented, or not, with 10 µM dopamine, L-DOPA, epinephrine, norepinephrine, or normetanephrine. Average values measured in CAA in the absence of any supplementation with siderophores are plotted against average values measured in CAA supplemented with either 10 µM catecholamines or normetanephrine. Median values represent the median of the relative intensity of each protein, normalized against all proteins detected by shotgun analysis (n = 3). The proteins of the pyochelin pathway are represented by yellow dots, those of the pyoverdine pathway by green dots, and the TBDTs by blue dots. B. Heat maps of various TBDTs and proteins involved in the pyochelin and pyoverdine iron uptake pathways: the darker the shade of blue, the higher the expression of the protein; the darker the shade of red, the more the expression of the protein is repressed. Only the proteins for which a change in the level of expression was observed are shown. FecA, FptA, FpvA, PA0434, PA3268, PfeA, PhuR, and PirA are TBDTs; FpvA, FpvC, PvdI, PvdL, and PvdQ are proteins of the pyoverdine-dependent

iron-uptake pathway; FptA, PchB, PchC, PchD, PchE, and PchF are proteins of the pyochelin-dependent iron-uptake pathway.

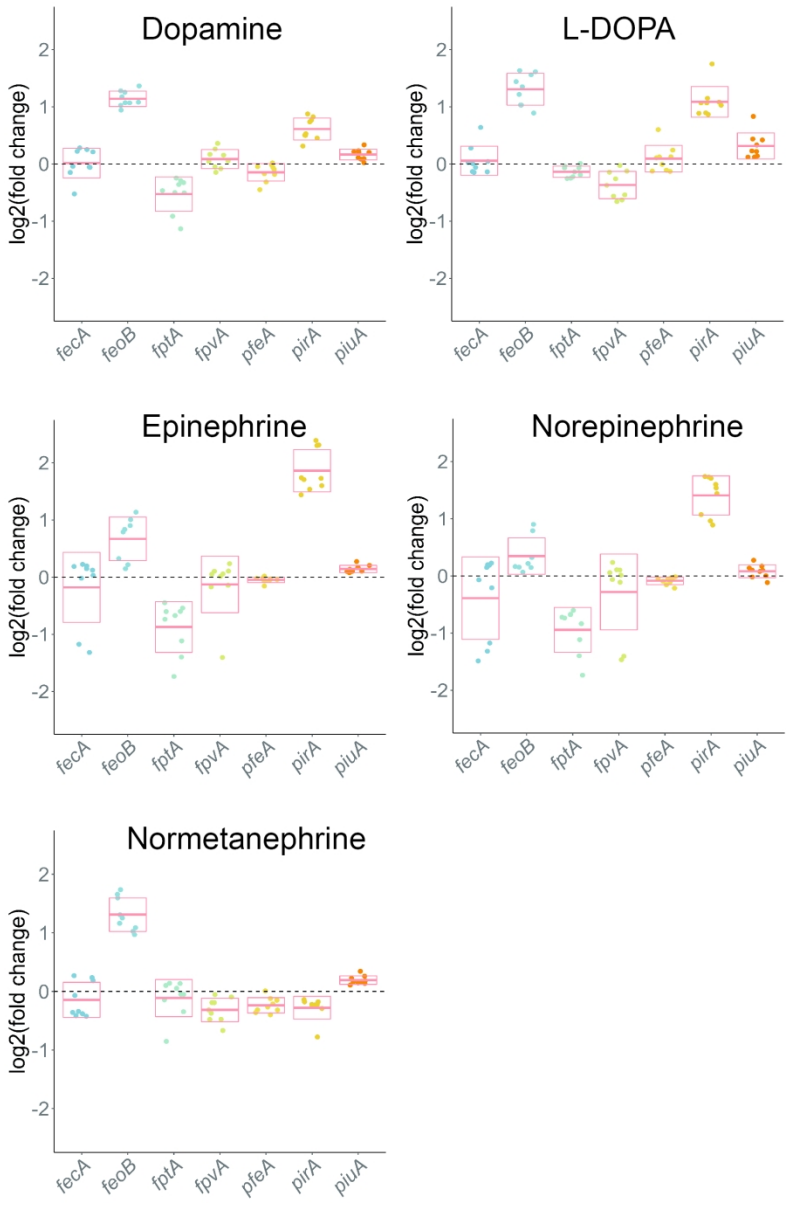

Figure 5. Analysis of changes in the transcription of genes encoding TBDTs involved in iron-uptake pathways in *P. aeruginosa* cells grown under iron-limited conditions (CAA medium) in the absence or presence of catecholamines. RT-qPCR was performed on pyoverdine- and pyochelin-deficient *P. aeruginosa* strains (Δ*pvdF*Δ*pchA*) grown in CAA medium for 8 h, as described in Materials and Methods, with or without 10 µM dopamine, L-DOPA, epinephrine, norepinephrine, and normetanephrine. The data were normalized relative to the reference gene *uvrD* and are representative of three independent experiments performed in triplicate (n = 3). Results are presented as the ratio between the values obtained in the presence of the catecholamines or normetanephrine over those obtained in their absence. fecA encodes the TBDT of ferri-citrate, *feoB* the ferrous inner membrane transporter, *fptA* and *fpvA* the TBDTs of pyochelin and pyoverdine, respectively, *pfeA* and *pirA* the TBDT of ENT, and *piuA* the TBDT of an unknown exosiderophore.

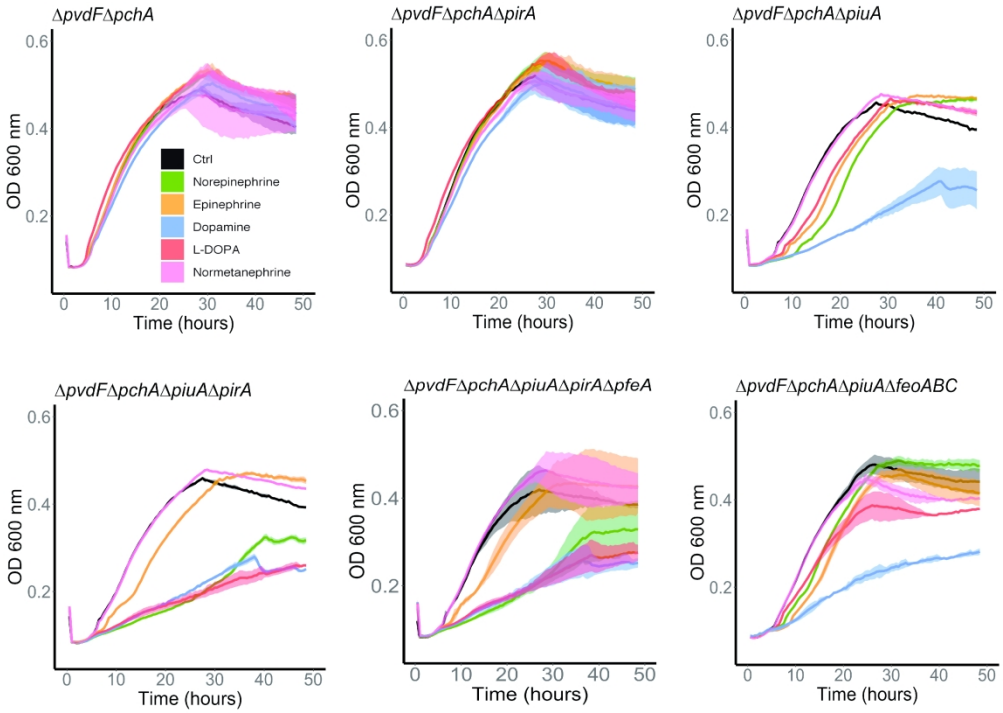

Figure 6. Growth of different *P. aeruginosa* TBDT mutants in the absence or presence of 10 µM catecholamines. The strains used are a pyoverdine and pyochelin mutant (Δ*pvdF*Δ*pchA*) and its corresponding TBDT deletion mutants. Strains were grown in CAA medium in the absence (Ctrl for control, kinetics in black) or presence of 10 µM catecholamines or normetanephrine. Growth was followed by monitoring optical density (OD) at 600 nm.

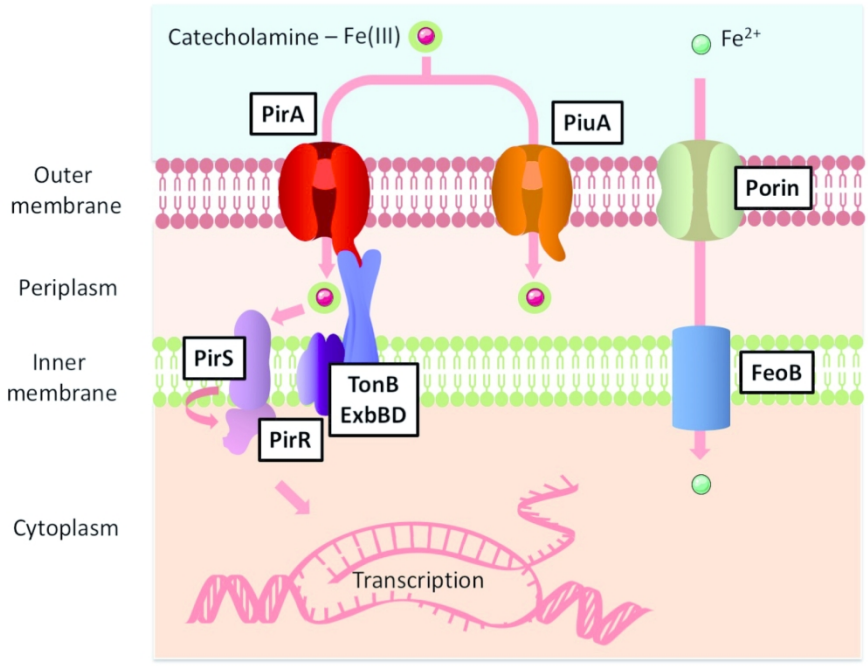

Figure 7: Transporters involved in iron acquisition by catecholamines in *P. aeruhinosa*. Catecholamines transport iron in *P. aeruhinosa* cells via the TBDTs PirA and PiuA. Catecholamine-Fe complexes are able to induce *pirA* transcription probably by interacting in the bacterial periplasm with the sensor of the two-component system PfeS/PirR (PirA being the transcriptional regulator). In the presence of L-DOPA, ferrous uptake is observed involving the FeoABC system.

159x121mm (300 x 300 DPI)